

‘Island Surfing’ Mechanism of Electron Acceleration During Magnetic Reconnection

M. Oka,¹ M. Fujimoto,² I. Shinohara,² T. D. Phan¹

Abstract. One of the key unresolved problems in the study of space plasmas is to explain the production of energetic electrons as magnetic field lines ‘reconnect’ and release energy in a explosive manner. Recent observations suggest possible roles played by small scale magnetic islands in the reconnection region, but their precise roles and the exact mechanism of electron energization have remained unclear. Here we show that secondary islands generated in the reconnection region are indeed efficient electron accelerators. We found that, when electrons are trapped inside the islands, they are energized continuously by the reconnection electric field prevalent in the reconnection diffusion region. The size and the propagation speed of the secondary islands are similar to those of islands observed in the magnetotail containing energetic electrons.

1. Introduction

The origin of energetic electrons of up to MeV in the Earth’s magnetotail has been an outstanding problem for decades [e.g. Sarris et al., 1976; Terasawa and Nishida, 1976]. Although many theories consider magnetic reconnection as the mechanism of explosive energy release phenomena in the Earth’s magnetosphere, the exact mechanism by which high energy electrons are produced is still unclear.

A statistical survey by the Geotail spacecraft shows that accelerated and/or heated electrons are more likely to be detected around the outflow regions somewhat away from the center of magnetic reconnection [Imada et al., 2005]. It was suggested that electrons pre-energized at the X-lines further gain energy in the flux pile-up region especially in the earthward side of the X-line. While a Cluster event at the near-Earth reconnection site also confirms this scenario [Imada et al., 2007], another event by the Wind spacecraft in the distant magnetotail observed increasing flux of energetic electrons with decreasing distance from the X-line, with no clear evidence for a flux pile-up region in the outflow jet, suggesting that the region around the X-line is the dominant source of energetic electrons [Øieroset et al., 2002]. The discrepancy between the two events is not well understood so far.

On the other hand, recent measurements by the Cluster spacecraft pointed out that magnetic islands may be an important agent responsible for the production of energetic electrons [Chen et al., 2008; Retinò et al., 2008]. The main features of the observed islands are that they are small - of the order of ion inertia length - and that they move fast, close to the Alfvén speed. These features suggest that they are the magnetic islands that are naturally formed as a consequence of secondary tearing instability of a thin current sheet [Eastwood et al., 2007, and references therein].

As for theoretical models of electron acceleration within magnetic islands, a contracting motion of volume filling magnetic islands has been considered [Drake et al., 2006].

Because of the contracting motion, inductive electric fields are created at each end of the islands and particles that are fast enough to circulate inside the islands can receive repetitive ‘kicks’ from the electric fields. However, the presence of volume filling islands and their contracting motion are difficult to verify observationally and have not been reported.

In this Paper, we present an alternative scenario of electron acceleration by performing 2D particle-in-cell (PIC) simulations of magnetic reconnection. We found that electrons are trapped in a secondary magnetic island so that they can be continuously energized by the reconnection electric field in the diffusion region.

2. Simulation

We utilize a two and half dimensional, fully relativistic PIC code [Hoshino, 1987; Shinohara et al., 2001]. The initial condition consists of two Harris current sheets. The anti-parallel magnetic field is given by $B_y/B_0 = \tanh((x - x_R)/D) - \tanh((x - x_L)/D) - 1$ where B_0 is the magnetic field at the inflow boundary, D is the half-thickness of the current sheet and L_x and L_y are the domain size in \hat{x} and \hat{y} direction, respectively. $x_L=L_x/4$ and $x_R=3L_x/4$ are the x -positions of the left and right current sheet, respectively. Periodic boundaries are used in both directions. The ion inertial length d_i is resolved by 25 cells. $D=0.5d_i$ and $L_x = L_y=102.4d_i$. The inflow, background plasma has the uniform density of $N_{B0}=0.2N_0$ where N_0 is the density at the current sheet center. The ion to electron temperature ratio is set to be $T_i/T_e=5$ for the current sheet and $T_i/T_e=1$ for the background. The background to current sheet temperature ratio $T_{bk}/T_{cs}=0.1$. The frequency ratio $\omega_{pe}/\Omega_{ce}=3$ where ω_{pe} and Ω_{ce} are the electron plasma frequency and the electron cyclotron frequency, respectively. The ion to electron mass ratio $m_i/m_e=25$ and the light speed c is $15V_A$ where V_A is the Alfvén speed defined as $B_0/\sqrt{4\pi N_0 m_i}$. We used average of 64 particles in each cell. 297 particles per cell represents the unit density.

No magnetic field perturbation is imposed at the beginning so that the system evolves from a tearing mode instability due to particle noise. Note that conventional simulations initiate magnetic reconnection by a small magnetic field perturbation in order to save computational time [e.g. Birn et al., 2001]. Our simulation setup does not use such trigger so that the system does not produce any large initial velocity flows resulting from a lack of pressure balance.

Figure 1a shows a snapshot of the out-of-plane component of electron current density $J_{e,z}$ obtained when the system is

¹Space Sciences Laboratory, University of California Berkeley, Berkeley, California, USA.

²Institute of Space and Astronautical Science, Japan Aerospace Exploration Agency, Sagami-hara, Kanagawa, Japan.

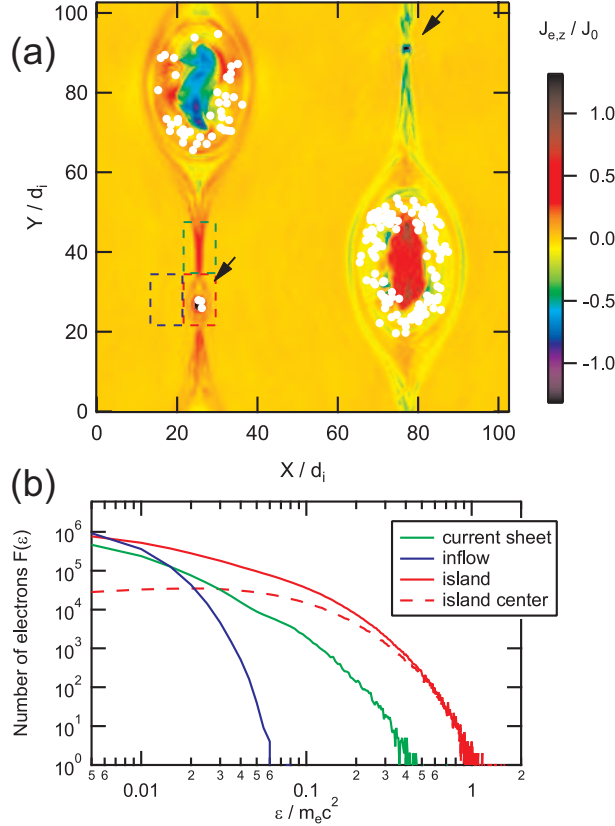


Figure 1. (a) The out-of-plane component of the electron current density at $\Omega_{ci}t=115$. Superposed on the image are the locations of the most energetic electrons ($\varepsilon > 1.4m_e c^2$). (b) Electron energy spectra integrated over the rectangular regions indicated in (a) (solid curves). The dashed curve shows the spectrum at a square region centered at $(x, y)=(25.6d_i, 26.4d_i)$ with each side $1.6d_i$.

well developed ($\Omega_{ci}t=115$). The diffusion regions are represented by the localized current densities in a thin current sheet, and embedded within the diffusion regions are the small scale secondary islands (highlighted by the arrows). Superposed on the plot are the locations of the most energetic electrons ($\varepsilon > 1.4m_e c^2$, indicated by the white circles). Most of the energetic electrons are located within the large islands but some electrons do exist in the small, secondary island of the left current sheet.

Those particles within the large islands are energized through the so-called multi-island coalescence resulting from the non-linear evolution of the tearing mode instability. A variety of different energization mechanisms has been found and they are fully described in our companion paper [Oka et al., 2010]. On the other hand, the energization of particles within the small islands are not the consequence of multi-island coalescence and the physics involved are entirely different, as will be shown below. Hereafter, we focus on the electron energization process within the small scale, secondary islands.

Figure 1b shows the electron energy spectra obtained at the time of Figure 1a. It is evident that, at $\Omega_{ci}t=115$, the highest energy electrons in the diffusion region are all confined in the small magnetic island, particularly at the very center of the island (red curves). This island overlaps the electron-scale diffusion region (or the so-called ‘inner diffusion region’) where electron acceleration should be efficient.

For a reference, we also plotted a spectrum for the immediate upstream (blue curve) and the downstream of this region (green curve).

In order to clarify the history of electron acceleration, we followed the trajectory of the highest energy electron in the rectangular box in Figure 1. In Figure 2, we divided the trajectory into five segments and plotted over the image that shows the out-of-plane component of the electron current density. Note that the simulation itself is two-dimensional in x and y but the displacement Δz can be calculated by integrating v_z over time. The background images are the snapshots taken from each segment so care should be taken when comparing the trajectory with the images. The y position as a function of energy ε is also shown in the right hand panel.

The secondary magnetic island starts to appear at $\Omega_{ci}t \sim 89$ (Figure 2a). The electron acceleration seen up until $\Omega_{ci}t \sim 89$ is what is typically seen in the inner diffusion region. Had the electron left the diffusion region upward soon after $\Omega_{ci}t \sim 89$, it would not have become one of the most energetic electrons in the system. In reality, it was deflected downward back to the diffusion region by the Lorentz force due to magnetic field of the emerging island. Then, a clear indication of the interaction between the electron and the secondary island is seen at $\Omega_{ci}t \sim 92$ (Figure 2b). A distinct change of the electron behavior starts at $\Omega_{ci}t \sim 95$. The electron is trapped in a well developed island (Figure 2c). The island continues to develop so that the magnetic island becomes as large as $\sim 5d_i$ although electron current is rather localized of the order of $2d_i$ (Figure 2d). During this later phase, the electron continues to gain energy constantly (Figure 2f).

The behavior of the electron can also be studied from the time profiles of the electromagnetic field felt by the particle (Figure 3b). Before being trapped by the island, the electron is rapidly energized by the strong ($\sim 0.1V_A B_0/c$) reconnection electric field. We confirmed that the work done by the E_z component, i.e. $(-e)\int v_z E_z dt$, dominates over the work done by the E_x and E_y components, i.e. $(-e)\int v_x E_x dt$ and $(-e)\int v_y E_y dt$.

Now, our interest goes to the next period during which the energy increases almost constantly until $\Omega_{ci}t \sim 110$ (Figure 3a). The energy increment is about $0.3m_e c^2$ and the displacement along the z direction is quite large, $\Delta z \sim 110d_i$. What is important here is that the island is expanding rather than contracting during the energization (Figure 2). Therefore, we must explore energization mechanism other than the contracting island mechanism [Drake et al., 2006]. After about $\Omega_{ci}t \sim 110$ when the island reaches the edge of the diffusion region, the energy remains almost constant at $\varepsilon \sim 1.5m_e c^2$.

The source of energy can again be studied from the profile of the electric field felt by the particle (Figure 3b). The x and y components of the electric field (to be discussed in more detail below) are oscillating so that the net energy gain from these components should be small. Here, we focus on the z component of the electric field, E_z , which is almost equivalent to the reconnection electric field. It remains, on average, constant at $E_z \sim 0.025V_A B_0/c$ until $\Omega_{ci}t \sim 110$ and then decreases to zero afterwards. Let us briefly check if this E_z can explain the energy increment $\Delta\varepsilon \sim 0.3m_e c^2$. Generally, the energy increase $\Delta\varepsilon$ is estimated as

$$\frac{\Delta\varepsilon}{m_e c^2} = \left(\frac{\Omega_{ce}}{\omega_{pe}}\right)^2 \left(\frac{cE}{V_A B_0}\right) \left(\frac{\Delta z}{d_i}\right) \quad (1)$$

where $\Omega_{ce}/\omega_{pe}=1/3$ in our simulation setup. For the particle we analyzed, it felt reconnection electric field $E_z \sim 0.025V_A B_0/c$ and was displaced $\Delta z \sim 110d_i$ during the

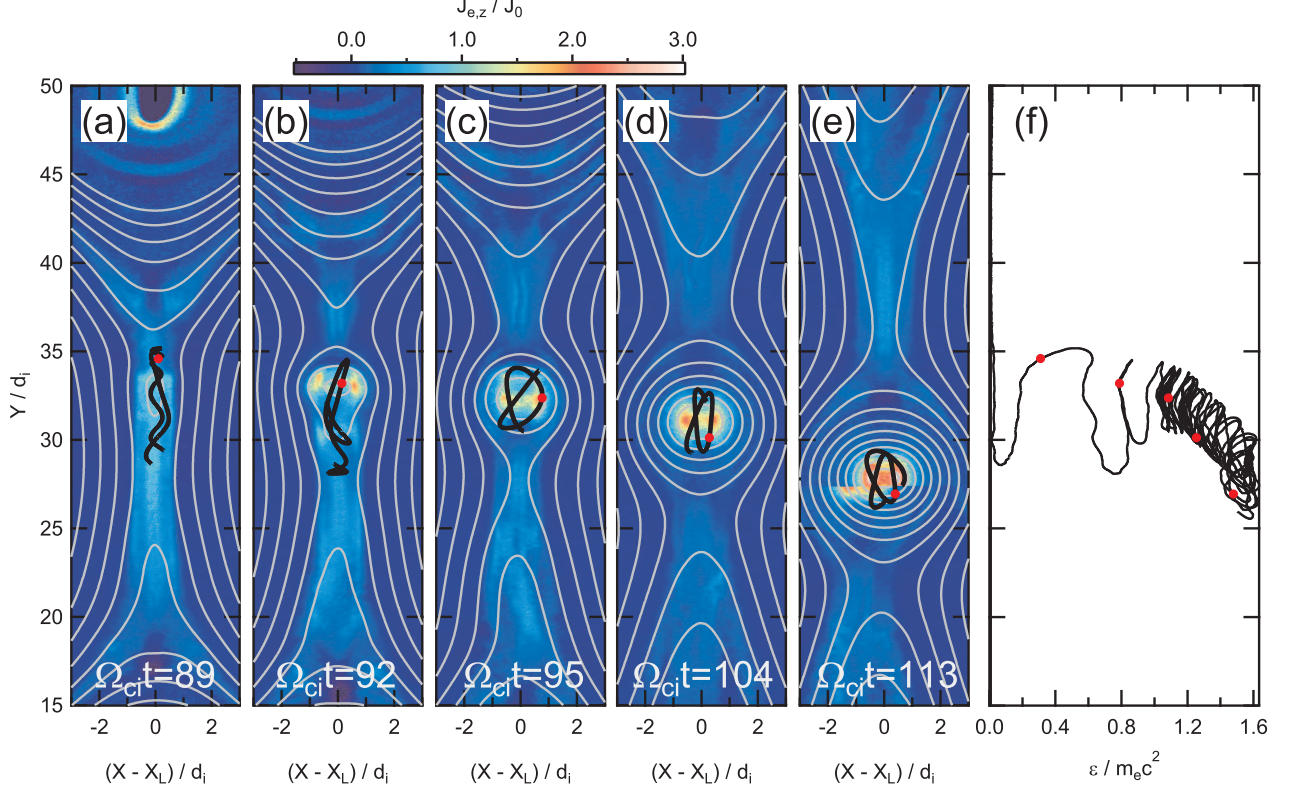


Figure 2. The trajectory of the most energetic electron during (a) $86.7 \leq \Omega_{ci}t \leq 90.7$, (b) $90.7 \leq \Omega_{ci}t \leq 93.3$, (c) $95.0 \leq \Omega_{ci}t \leq 95.6$, (d) $103.7 \leq \Omega_{ci}t \leq 104.3$, (e) $112.4 \leq \Omega_{ci}t \leq 113.0$. The background images are the electron current density at (a) $\Omega_{ci}t=88.7$ (b) $\Omega_{ci}t=92.0$, (c) $\Omega_{ci}t=95.3$, (c) $\Omega_{ci}t=104.0$, and (d) $\Omega_{ci}t=112.7$. In (e), the whole trajectory ($0 \leq \Omega_{ci}t \leq 115$) is shown in a format of y versus ε . Each red mark shows the time of the background image.

period $100 \leq \Omega_{ci}t \leq 110$ so that the energy increment should be $\Delta\varepsilon \sim 0.3m_e c^2$ in agreement with the above measured value. From these arguments, we conclude that the electron is energized by the reconnection electric field E_z while being trapped within the secondary island.

One may point out a possibility of adiabatic heating because the magnetic field magnitude shows gradual increase during the energization (Figure 3c). However, this is not the case. The spatial scale of the particle motion is comparable to the island size so that the trajectory is decoupled from the magnetic field lines, indicating that the electron is highly non-adiabatic (Figure 2c-e). We also confirmed that the magnetic moment μ of this particle is not constant during the energization (not shown).

The main feature of the secondary magnetic island within a diffusion region is that it contains an electrostatic potential well. In the diffusion region, ions are unmagnetized while electrons are more magnetized so that the in-plane, polarization electric field E_p is generated and converge toward the center of the magnetic island.

Figure 4a and Figure 4b respectively shows the potential and the electromagnetic field structure at and around the secondary magnetic island shown in Figure 2c. It is evident that the potential well exists in the magnetic island and that its depth is of the order of the kinetic energy of the reconnection outflow $\Phi \sim m_i V_A^2$. The deep potential well is represented by the large, bipolar signature in the E_y profile. A small bipolar signature also appears in the otherwise flat profile of E_z because of the motion of the entire island with the speed $\sim 0.3V_A$ directed toward the negative y -direction. This structure led to the oscillatory profile of the E_z felt by the particle (Figure 2f). Note again that the net energy gain is positive because of the E_z offset due to the reconnection electric field.

3. Discussion

We found an energization mechanism by which electrons are trapped by a small scale magnetic island so that they are continuously energized by the reconnection electric field within the diffusion region. This is similar to the ‘surfing’ mechanism by which electrons are accelerated by the reconnection electric field while ‘surfing’ along the layer of the in-plane, polarization electric field [Hoshino, 2005]. In order to discriminate the two mechanisms, we term the newly found mechanism as the ‘island surfing’. Let us now consider the ‘island surfing’ in a similar way as discussed by Hoshino [2005]. As an example, we consider an electron that is located along the current sheet center ($x=x_L$) but slightly away from the island center (Figure 4c). From the symmetry of the electromagnetic fields at and around the magnetic islands, the following arguments can be applied to other electrons without losing generality. The y -component of the equation of motion reads

$$\frac{dp_y}{dt} = (-e)E_y + \left(-\frac{e}{c}\right)(v_z B_x - v_x B_y) \quad (2)$$

where $p_y = m_e v_y$ is the electron momentum, E_y on the right-hand side can be replaced by the polarization electric field E_p produced within the magnetic island, and the guide field $B_y = 0$ in the present case. If the Lorentz force $F_B = (-e/c)v_z B_x$ is larger than the electric force $F_E = (-e)E_p$, the electron is trapped and will gain energy from the reconnection electric field E_z . From the trapping condition, we get

$$|v_z| > c \frac{E_p}{B_x} \sim \left(\frac{d_i}{l}\right) V_A \quad (3)$$

indicating that the ‘island surfing’ mechanism requires a pre-acceleration to be kept trapped within an island. In general, the polarization electric field E_p is expressed as

$$\frac{E_p}{B_0 V_A/c} = \frac{d_i}{l} \quad (4)$$

where l is the thickness of the potential structure and may be estimated as an intermediate scale between ion inertia and the electron inertia length, $l = c/\sqrt{\omega_{pe}\omega_{pi}}$ [Hoshino, 2005]. In the present case, l is measured from the radius of the secondary island and is of the order of the ion inertial length. This is not unrealistic because the size (diameter) of the magnetic islands observed by the Cluster spacecraft was about two times the ion inertia length [Chen et al., 2008]. For B_x , we can assume to be a minor factor smaller than B_0 from our simulation result. Then, the minimum value of $|v_z|$ is a minor factor larger than V_A . This is not a serious condition given the fact that electrons have a great chance of pre-acceleration at the X-line as we have already seen in Figure 2a. Note also that, in the region away from the X-line but within the diffusion region, electrons can be bulk accelerated up to $V_{Ae} = \sqrt{m_i/m_e} V_A$ [e.g. Hoshino et al., 2001].

An accelerated electron would be kept trapped as long as its gyro-radius $r_L = p_e/eB_l$ remains smaller than the size of the structure R where p_e is the electron momentum and B_l is the local magnetic field magnitude felt by the particle. Since magnetic field lines of the inflowing plasma constantly accumulate on the island, we may assume that the size increases with the rate $\alpha_r V_A$ where α_r is the instant reconnection rate. For the initial size of the magnetic island R_0 and the time from the start of the island expansion Δt , $R = R_0 + \alpha_r V_A \Delta t$. Then, the trapping condition $r_L < R$ can

be rewritten as

$$\frac{p_e}{m_e c} < \sqrt{\frac{m_i}{m_e}} \left(\frac{B_l}{B_0}\right) \left(\frac{\Omega_{ce}}{\omega_{pe}}\right) \left(\frac{R_0}{d_i} + \alpha_r \Omega_{ci} \Delta t\right) \quad (5)$$

but $R_0 > d_i$, $\omega_{pe} > \Omega_{ci}$ and $B_l/B_0 \sim 1$ in our simulation and in the magnetotail as well so that the maximum velocity would be

$$v_{z,\max} \sim c \quad (6)$$

in the non-relativistic regime, indicating ‘unlimited’ electron acceleration by the ‘island surfing’ mechanism (If the electron is actually energized up to a relativistic energy, equation (5) gives the upper limit). This efficient acceleration is an advantage of the closed field line geometry of the secondary islands.

Note, however, that the ‘island surfing’ works only for the island located within the diffusion region entirely covered by the reconnection electric field (Figure 4c). Any other island outside the diffusion region lacks the reconnection electric field and has to generate motional electric field to accelerate electrons. This can only be achieved by a contracting motion (Figure 4d). A bulk motion of the entire island does not accelerate electrons because it generates a positive out-of-plane electric field at one end and a negative out-of-plane electric field at the other end, resulting in a small, net energy gain.

In our simulation, the electron in Figure 2 and 3 has already reached $\varepsilon/m_e c^2 = 1$ with the displacement of $\Delta z/d_i \sim 150$ during the initial interaction of the newly emerging island. Note that we used an unrealistically high initial temperature $\varepsilon_{th} = 9.2 \times 10^{-3} m_e c^2 \sim 4.7$ keV due to limited computational resources. If we normalize simulated particle energies by ε_{th} which is ~ 1 keV in the magnetotail and assume $d_i = 500$ km, the simulation indicates electron energization up to 110 keV with the dawnward displacement $\sim 12R_E$. Given the fact that the diameter of the magnetotail is $\sim 40R_E$, the initial interaction with the emerging secondary island may explain energetic (< 127 keV) electrons observed by the Cluster spacecraft that passed through small scale magnetic islands [Chen et al., 2008].

The main part of the ‘island surfing’ may work in much larger scale current sheets such as those found in the solar atmosphere. In this respect, we would also like to point out that magnetic reconnection in a spatially large current sheet (in the y -direction) would yield not just one magnetic island but a chain of islands [Loureiro et al., 2007] so that a multitude of ‘island surfing’ builds up to create a significant amount of energetic electrons. In addition, if an external force existed to drive the magnetic reconnection, the reconnection electric field increases [Hoshino, 2005] and the frequency of secondary island generation also increases [Wan and Lapenta, 2008]. Such a driven configuration is favorable for more energization by the ‘island surfing’.

We did not consider a guide field, but our preliminary simulation with a guide field ($B_g = 0.3B_0$) also showed efficient electron energization within a secondary magnetic island, although its efficiency is still under investigation.

Finally, we would like to point out that the ‘island surfing’ is not just a matter of energization of a few unusual electrons. It would give an insight toward the understanding of the roles of secondary islands in the context of energy dissipation during magnetic reconnection.

Acknowledgments. Simulations are performed on the SX-9 computer of ISAS, JAXA, Japan. We thank helpful comments from M. Swisdak.

References

Birn, J. et al. (2001), Geospace Environmental Modeling (GEM) Magnetic Reconnection Challenge, *J. Geophys. Res.*, *106*, 3715-3719.

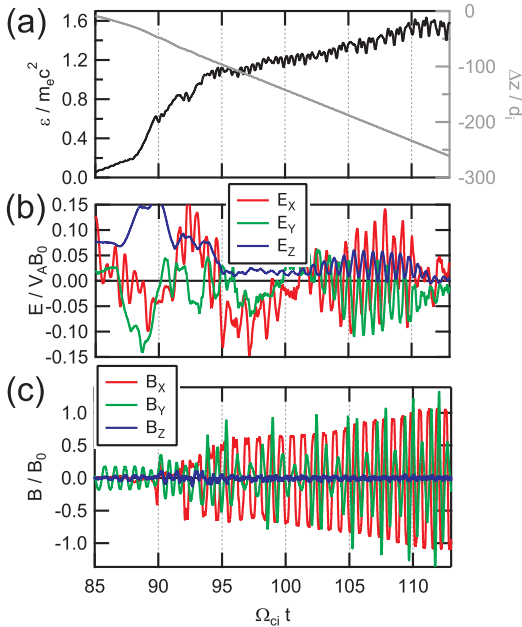


Figure 3. Time profiles of (a) the energy and the displacement Δz , (b) the electric field and (c) the magnetic field felt by the particle during the trapping motion. In order to eliminate the particle noise, the electric field data have been smoothed by box average with the box size of $\Omega_{ci} \Delta t = 2.7$.

Chen, L. -J., Bhattacharjee, A., Puhl-Quinn, P. A., Yang, H., Bessho, N., Imaga, S. et al. (2008), Observation of energetic electrons within magnetic islands, *Nature Phys.* 4, doi:10.1030/nphys777.

Drake, J. F., Swisdak, M., Che, H. and Shay, M. A. (2006), Electron acceleration from contracting magnetic islands during reconnection, *Nature*, 443, —doi:10.1038/nature05116.

Eastwood, J. P., T.-D. Phan, F. S. Mozer, M. A. Shay, M. Fujimoto, A. Retinò, M. Hesse et al. (2007), Multi-point observations of the Hall electromagnetic field and secondary island formation during magnetic reconnection, *J. Geophys. Res.*, 112, A06235.

Hoshino, M. (1987), The electrostatic effect for the collisionless tearing mode, *J. Geophys. Res.*, 92, 7368-7380.

Hoshino, M., Mukai, T., Terasawa, T. and Shinohara, I. (2001), Suprathermal electron acceleration in magnetic reconnection, *J. Geophys. Res.*, 106, 25979-25997.

Hoshino, M. (2005), Electron surfing acceleration in magnetic reconnection, *J. Geophys. Res.*, 110, A10215.

Imada, S., Hoshino, M., and Mukai, T. (2005), Average profiles of energetic and thermal electrons in the magnetotail reconnection regions, *Geophys. Res. Lett.*, 32, L09101.

Imada, S., Nakamura, R., Daly, P. W., Hoshino, M., Baumjohann, W., Mühlbacher, S., Balogh, A., et al. (2007), Energetic electron acceleration in the downstream reconnection outflow region, *J. Geophys. Res.*, 112, A03202.

Loureiro, N. F., A. A. Schekochihin and S. C. Cowley (2007), Instability of current sheets and formation of plasmoid chains, *Phys. Plasmas*, 14, 100703.

Oka, M., Phan, T., Krucker, S., Fujimoto, M. and Shinohara, I. (2010), Electron acceleration by multi-island coalescence, *Astrophys. J.*, , in press.

Øieroset, M., Lin, R. P., Phan, T. D., Larson, D. E. & Bale, S. D. (2002), Evidence for Electron Acceleration up to ~ 300 keV in the Magnetic Reconnection Diffusion Region of Earth's Magnetotail, *Phys. Rev. Lett.*, 89(19), 195001.

Pritchett, P. L. (2008), Energetic electron acceleration during multi-island coalescence, *Phys. Plasmas*, 15, 102105.

Retinò, A., Nakamura, R., Vaivads, A., Khotyaintsev, Y., Hayakawa, T., Tanaka, K., Kasahara, S. et al. (2008), Cluster observations of energetic electrons and electromagnetic fields within a reconnecting thin current sheet in the Earth's magnetotail, *J. Geophys. Res.*, 113, A12215.

Sarris, E. T., S. M. Krimigis and T. P. Armstrong (1976), Observations of Magnetospheric Bursts of High-Energy Protons and Electrons at $\sim 35 R_E$ with Imp 7, *J. Geophys. Res.*, 81(13), 2341-2355.

Shinohara, I. et al. 2001, *Phys. Rev. Lett.*, 87, 095001

Terasawa, T. and A. Nishida (1976), Simultaneous observations of relativistic electron bursts and neutral-line signatures in the magnetotail, *Planet. Space Sci.*, 24, 855-866.

Wan, W. and G. Lapenta (2008), Electron Self-Reinforcing Process of Magnetic Reconnection, *Phys. Rev. Lett.*, 101, 015001.

M. Oka, T. D. Phan, Space Sciences Laboratory, University of California Berkeley, 7 Gauss Way Berkeley, CA 94720-7450, USA. (moka@ssl.berkeley.edu)

M. Fujimoto, I. Shinohara Institute of Space and Astronautical Science, Japan Aerospace Exploration Agency, 3-1-1 Yoshinodai, Sagami-hara, Kanagawa, 229-8510, Japan.

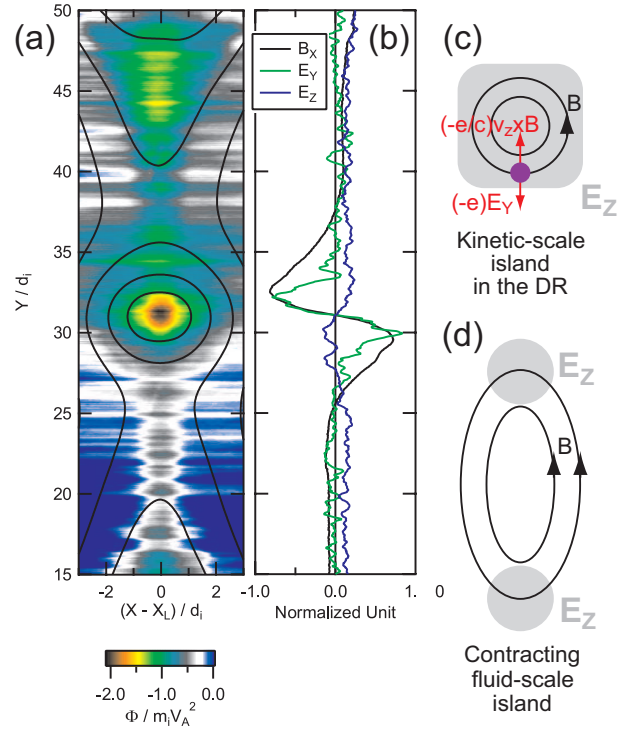


Figure 4. (a) The electric potential at $\Omega_{ci}t=104$. The contour shows the magnetic field lines. (b) A 1D cut through $x = x_L$ of B_x/B_0 , $cE_y/V_A B_0$, and $cE_z/V_A B_0$. (c) A schematic illustrations of a secondary island in the diffusion region (DR) and the force balance of an electron. (d) An illustration of a contracting island.